CORE
Metadata, citation and similar papers at core.ac.uk
Provided by CERN Document Server

TE-MSC

CERN TE-Note-2010-04

attilio.milanese@cern.ch

EDMS no : 1057916

# Shapes of coil ends in racetrack layout for superconducting magnets

Attilio Milanese / TE-MSC department

Keywords: racetrack coils, coil winding, least energy curve, smooth curve, superconducting magnets

## Summary

Racetrack coils have received considerable attention for $Nb_3Sn$ magnets, both built using the React-and-Wind and Wind-and-React techniques. The geometry usually consists of a series of straight parts connected with circular arcs. Therefore, at the interface between these sections, a finite change in curvature is imposed on the cable. Alternative transition curves are analyzed here, with a particular focus on the total strain energy and the minimum / maximum radii of curvature. The study is presented in dimensionless form and the various alternatives are detailed in mathematical terms, so to be used for drafting or simulations. Extensions for the design of flared ends are also briefly discussed.

This study is within the framework of the EuCARD WP7-HFM project. In particular, the proposed curve can be used for the end design of the high field model magnet (Task 7.3).

## 1. Introduction

The racetrack configuration has been recently employed for several Nb3Sn coils wound with Rutherford cables: see, for example, the common coils dipoles designed at BNL [1], FNL [2] and LBNL [3], the HD1 [4] and CERN SMC [5]. Moreover, LBNL designed, built and tested HD2 [6], a dipole with racetrack ends that flare out to clear a circular aperture. The geometry of the coil is shown in Fig. 1, together with a picture taken during coil winding [7].

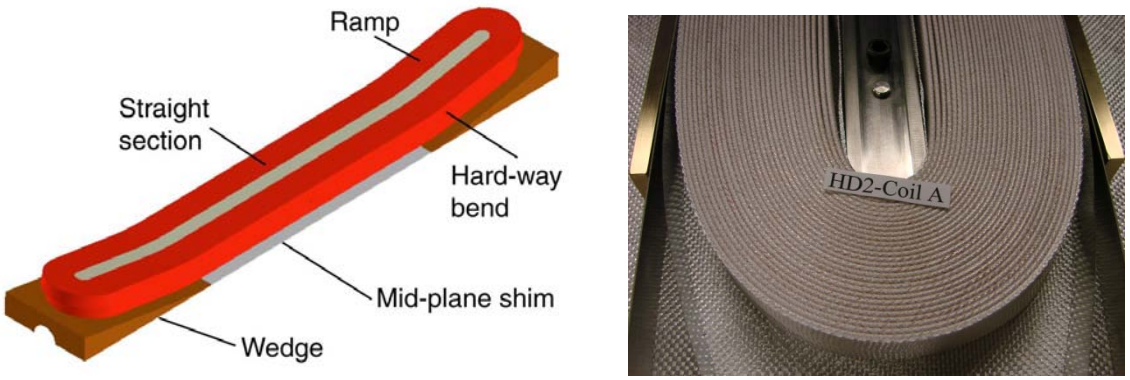


Figure 1. Coil geometry (left) and picture of a coil after winding (right), for HD2.

This is an internal CERN publication and does not necessarily reflect the views of the management

Focusing in particular on HD2, each cable turn – not considering the special case when a layer jump occurs – involves the following geometric pattern:

a) straight section parallel to the midplane of the magnet

b) circular arc in a plane containing the cable (hard-way bend)

c) straight section on an inclined plane

d) circular semicircle on a plane orthogonal to the cable (easy-way bend)

e) straight section on an inclined plane

f) circular arc in a plane containing the cable (hard-way bend)

For a purely racetrack configuration, the pattern consists of points a) and d) alone.

Although such a geometry is inherently simple and well suited for the mechanical design, it has the drawback of generating discontinuities on the curvature of the cable. Looking at the flared end geometric pattern, the cable has zero curvature in parts a), c) and e), while it has a finite one in the circular parts. If the assumption is made that the cable can be modelled using classical beam theory, an instantaneous jump in curvature corresponds to a concentrated moment on the cable: this cannot be provided by the surrounding support structure. Hence, the cable is likely to follow the imposed geometry reluctantly.

This effect can be seen in Fig. 1: the first turn around the pole island exhibits a tendency to lift off and the first turns appear somehow loose. This phenomenon has been observed also with other magnets. For the particular case of HD2, where both a hard-way and easy-way bend are present, the magnetic tests show that the quenches originate in the straight section parts parallel to the midplane, and all within the last 100 mm before the hard-way bend [6].

These drawbacks motivate the study of transition curves to be used instead of traditional straight-circular arc couples in racetrack type coils. A good candidate transition curve should satisfy the following constraints:

- not be too long, as to limit the end region
- be smooth up to the second derivative, to ensure continuity of the curvature
- be convex, since a non-convex baseline cannot be conveniently used for winding purposes
- minimize the total strain energy
- avoid localized peaks of strain energy (i.e., maximize the minimum bending radius)

The mathematical problem can be stated, with reference to Fig. 2, as follows: connect points A = (0,0) and B = ($h$,1) with a curve having horizontal tangent in A and vertical tangent in B. The $y$ coordinate of B is chosen to be unitary as to work in dimensionless terms; the $x$ coordinate of B is left free. The curve continues straight to the left of A (straight part of cable), while it mirrors above B (symmetric coil). Therefore, it would be preferable to have zero curvature at A and a finite one at B.

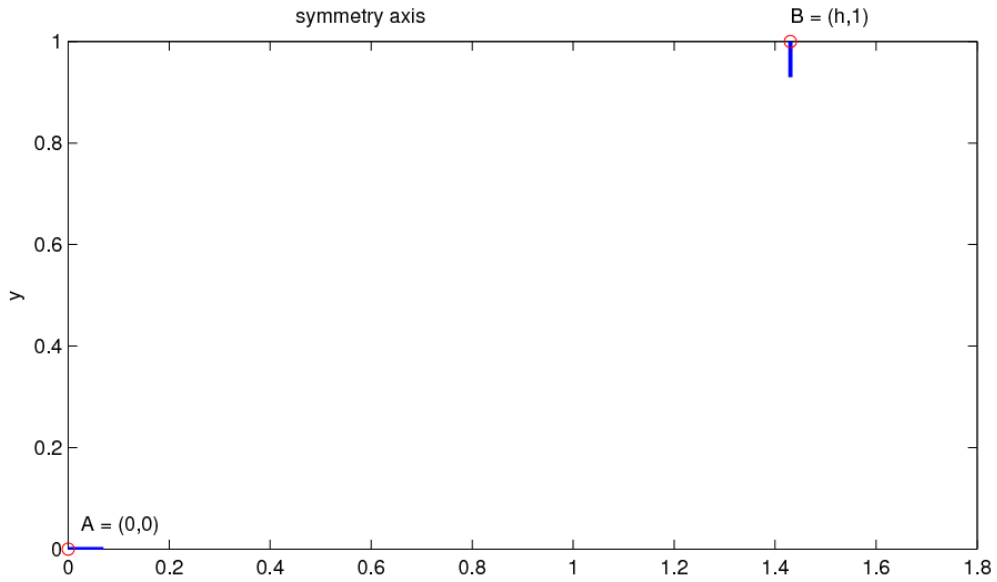


Figure 2. Geometry of the planar problem: two points need to be properly connected.

If $t$ is a real parameter, the curve can be represented as

$$\begin{cases} x = x(t) \\ y = y(t) \end{cases} \qquad 0 \le t \le t_{max}$$

The curvature $k$ along the curves can be defined as

$$k(t) = \frac{1}{R(t)} = \frac{|x'y'' - y'x''|}{(x'^2 + y'^2)^{3/2}}$$

where the primes indicate derivative with respect to $t$, and $R(t)$ is the radius of curvature. The differential distance along the curve $ds$ is

$$ds = \sqrt{x'^2 + y'^2}\,dt$$

The physical interpretation of $R$ and its connection with the change in tangent angle $\theta$ are shown in Fig. 3. From that – and considering that $\theta$ can either increase or decrease – it is immediate to derive

$$\left|\frac{d\theta}{ds}\right| = \frac{1}{|R|} = k$$

The strain energy is proportional to the square of the curvature. Hence, omitting the proportionality factor, the total strain energy $E$ is

$$E = \int_0^L [k(s)]^2 ds = \int_0^{t_{max}} \left[\frac{|x'y'' - y'x''|}{(x'^2 + y'^2)^{3/2}}\right]^2 \sqrt{x'^2 + y'^2}\,dt = \int_0^{t_{max}} \frac{(x'y'' - y'x'')^2}{(x'^2 + y'^2)^{5/2}}\,dt$$

where $L$ is the curve length. This expression gives the integrated strain energy obtained using classical beam theory, under the assumption that the undeformed beam is straight.

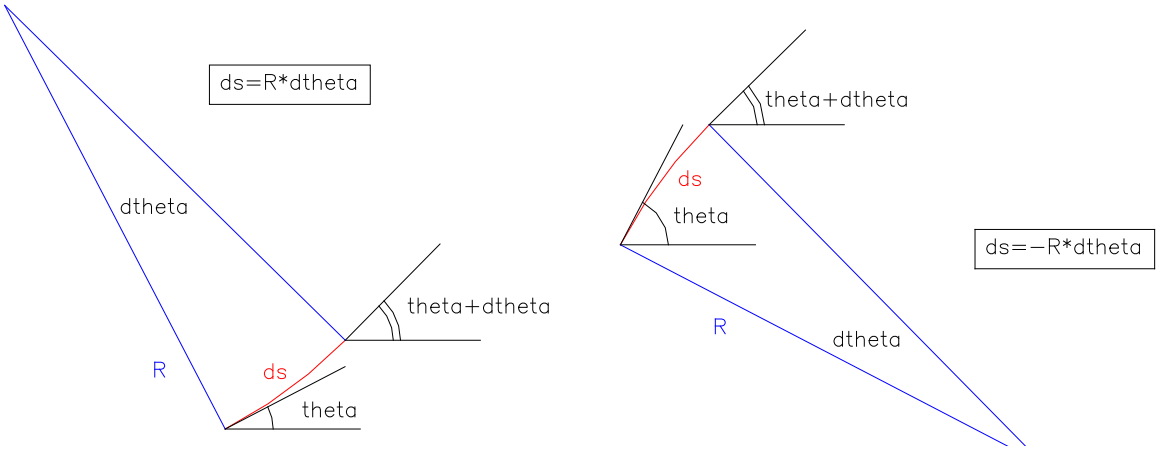


Figure 3. Geometric interpretation of the curvature.

In the following, several curves are discussed and detailed. The general problem of finding the curve that minimizes the total strain energy is not new: it has been solved, for example, by Euler in the 18th century [8]. Modern solutions are presented in [9] and [10]. Cases not found in the literature – dictated by the practical needs motivating this study – are presented and solved as well.

The curves detailed here are planar and as such they can be directly used as baselines for the design of racetrack ends. However, the same concepts can be extended in three dimensional space. For example, considering a racetrack flared end of the HD2 type, transition curves can be used in both the hard- and easy-way bends.

## 2. Circular arc

As a reference, the case of a circular arc is reported first. The analysis is trivial but useful, also because it sets the stage for comparisons. The solution is reported in Fig. 4.

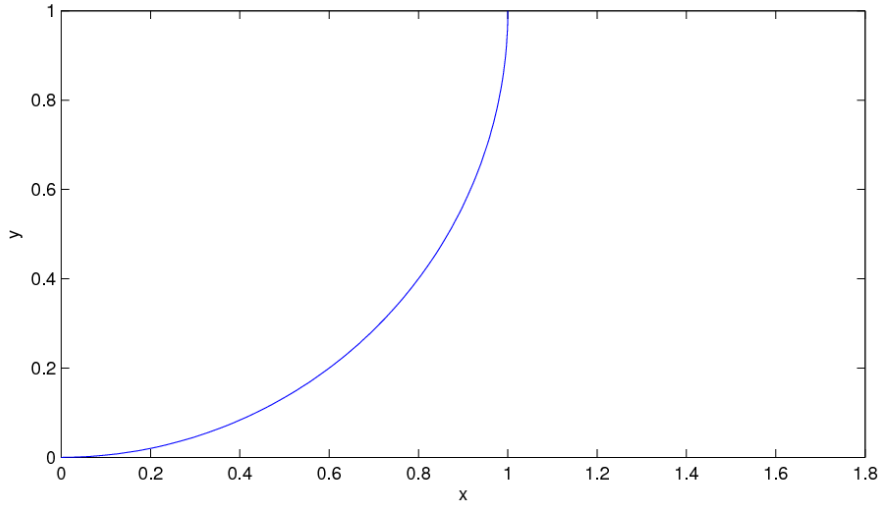


$$h = 1$$

$$L = \frac{\pi}{2}$$

$$E = \frac{\pi}{2}$$

$$R_{min} = 1$$

$$R_{max} = 1$$

Figure 4. Circular arc.

The radius of curvature is everywhere constant and equal to 1. Plots of the curvature *k* vs. the distance *s* along the curve, as well as vs. the horizontal coordinate *x*, are reported in Fig. 5.

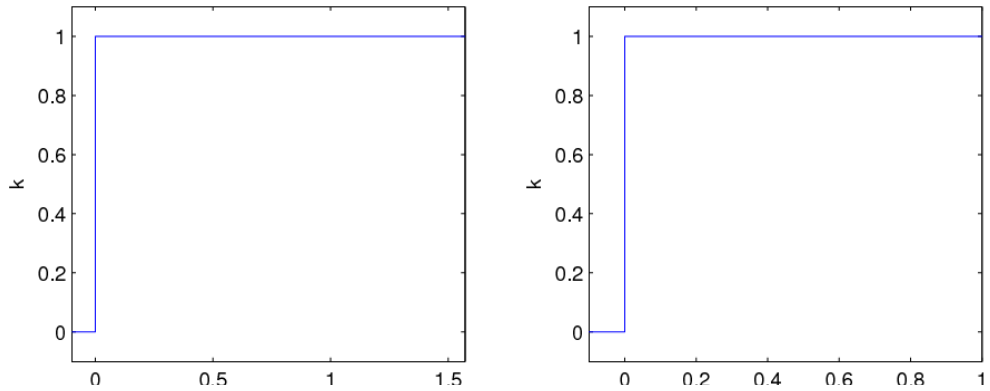


Figure 5. Curvature $k(s)$ and $k(x)$ for a circular arc.

The curvature is discontinuous at the beginning of the curve, where the arc meets the straight line.

## 3. Elliptic arc

The elliptic arc is considered here. With respect to Fig. 2, the semi-axes are $h$ and 1, along the $x$ and $y$ axes, respectively. Since $h$ is a variable, it can be chosen as to minimize the total strain energy $E$.

Writing the parametric equation of a 90° elliptic arc as

$$\begin{cases} x = h \sin t \\ y = 1 - \cos t \end{cases} \qquad 0 \le t \le \frac{\pi}{2}$$

then the energy is a function of $h$,

$$E(h) = \int_0^L [k(s)]^2 ds = \int_0^{\pi/2} \frac{h^2}{[\sin^2 t - h^2(\sin^2 t - 1)]^{5/2}} dt$$

For a fixed value of $h$, the above integral can be solved using numerical quadrature; then, the minimum can be found using a unidimensional minimization algorithm. For convenience, the MATLAB functions “quadgk” and “fminbnd” [11] are used here. The solution is shown in Fig. 6.

The values of $h$, $L$ and $E$ reported above coincide with those of [9]. The curvature $k$ as a function of $s$ and $x$ is reported in Fig. 7.

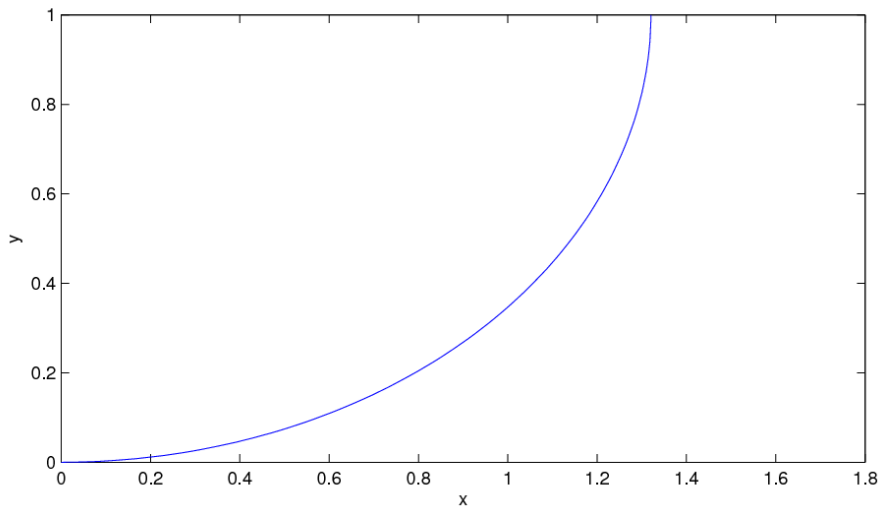


$$h = 1.3204$$

$$L = 1.1657 \cdot \frac{\pi}{2}$$

$$E = 0.9342 \cdot \frac{\pi}{2}$$

$$R_{min} = \frac{1^2}{h} = = 0.7573$$

$$R_{max} = \frac{h^2}{1} = = 1.7435$$

Figure 6. Least energy elliptic arc.

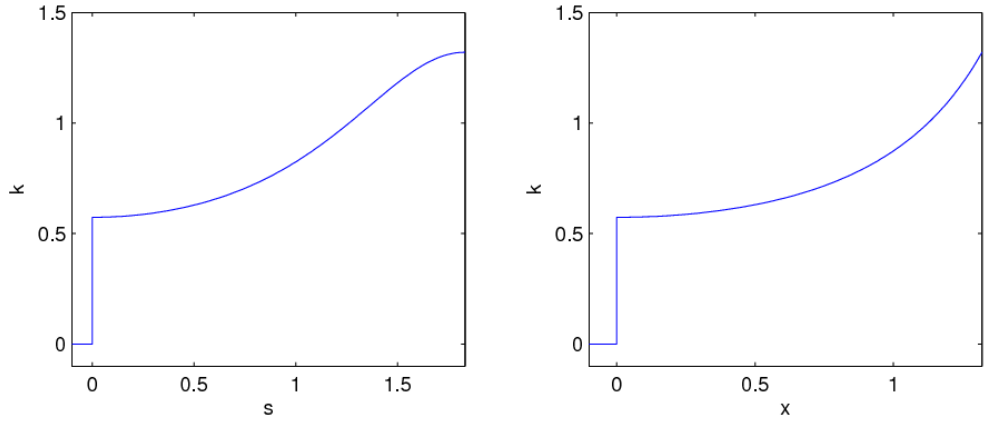


Figure 7. Curvature $k(s)$ and $k(x)$ for the least energy elliptic arc.

This elliptic curve still involves a finite change in curvature where the arc meets the straight line. The radius of curvature decreases along the curve, reaching a minimum at the end of the arc. The total strain energy is smaller than the one of the circular option, though the peak strain energy increases. Finally, this elliptic curve is longer than the circular arc.

## 4. Superelliptic arc

The parametric equations of a 90° superelliptic arc from point A to B of Fig. 2 are

$$\begin{cases} x = h[\sin t]^{2/m} \\ y = 1 - [\cos t]^{2/n} \end{cases} \qquad 0 \le t \le \frac{\pi}{2}$$

This curve can be viewed as a generalization of the ellipse, that is found by setting the exponents $m = n = 2$. In the particular case when $m = n$, a hyperelliptic arc is obtained. To ensure that the tangents in A and B are as required, both $m$ and $n$ shall be greater than 1.

In this case, there are three variables that can be tuned to minimize the total strain energy $E$, i.e., $h$ (as in the elliptic case) and the two exponents $m$ and $n$. Hence, a curve with an $E$ at least as small as in the previous case shall be found. Writing $E = E(h,m,n)$ as the integral of the square of the curvature returns a lengthy expression. However, a numerical solution is still feasible, coupling a quadrature scheme to an optimizer. The solution obtained is $m = 2.75$, $n = 1.99$ and is illustrated in Fig. 8. The superelliptic case is not analyzed in [9].

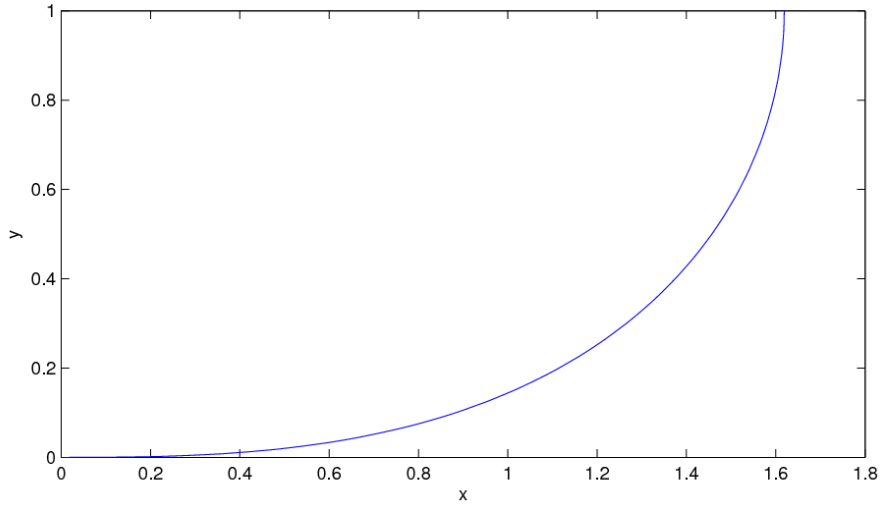


$$h = 1.6189$$

$$L = 1.3278 \cdot \frac{\pi}{2}$$

$$E = 0.9140 \cdot \frac{\pi}{2}$$

$$R_{min} = 0.8440$$

$$R_{max} = \infty$$

Figure 8. Least energy superelliptic arc.

As expected, the total strain energy is (slightly) lower than in the case of the elliptic arc, although the curve is (considerably) longer in the $x$ direction. An advantage of this solution is, however, that the curvature is 0 where the arc connects to the straight part: hence, it involves a smooth transition. Furthermore, the minimum bending radius is larger than the one occurring in the elliptic solution.

The dependence of the curvature $k$ on the distance $s$ and coordinate $x$ is reported in Fig. 9. Looking at $k(s)$, the curvature increases almost linearly with the distance for almost three quarters of the arc, then it veers down. Interestingly, if $k(x)$ is plotted, an almost linear behaviour is observed throughout the curve. Hence, it could be inferred that when more free parameters are inserted into the curve (in this case, $h$, $m$ and $n$), minimizing the total strain energy *de facto* pushes $k(x)$ to be linear.

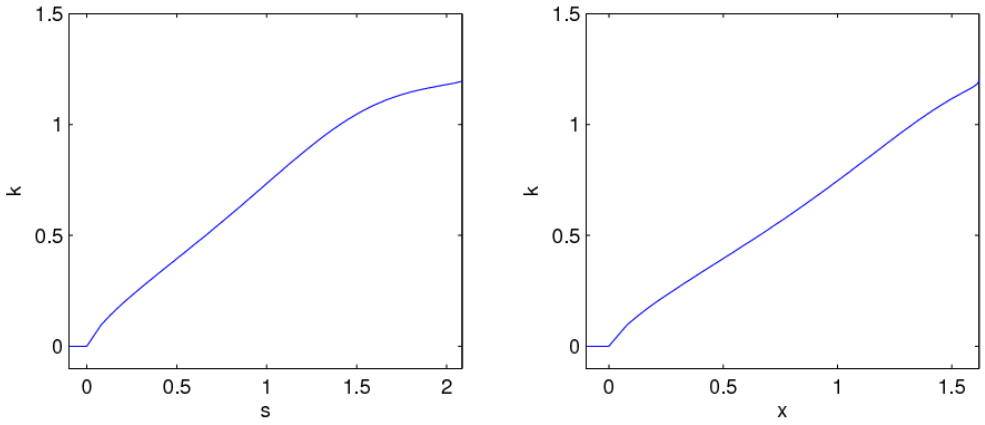


Figure 9. Curvature $k(s)$ and $k(x)$ for the least energy superelliptic arc.

## 5. Clothoid

The next candidate is – quite naturally – the clothoid. Such a curve is also known as Cornu spiral or Euler spiral. It is defined as a curve in which the curvature varies linearly along the distance. It finds application, for example, in the design of road and railroad turns, to smoothen the effects of a sudden centripetal acceleration on the vehicles and their passengers.

The parametric equations, using a regular parametrization, are derived next. The general case of a curve connecting points A and B with tangents $\theta_A$ and $\theta_B$ and radii of curvature $R_A$ and $R_B$ is considered first. By definition of the clothoid, the curvature $k(s)$ is

$$k(s) = \frac{1}{R(s)} = \frac{d\theta(s)}{ds} = k_1 s + k_2$$

Hence,

$$d\theta = (k_1 s + k_2) ds$$

and

$$\theta(s) = \frac{1}{2} k_1 s^2 + k_2 s + \theta_A$$

The constants $k_1$ and $k_2$ can be derived from the initial and final radii of curvature, as

$$k(s = 0) = k_2 = \frac{1}{R_A}$$

$$k(s = L) = k_1 L + k_2 = k_1 L + \frac{1}{R_A} = \frac{1}{R_B}, \qquad k_1 = \frac{1}{L}\left(\frac{1}{R_B} - \frac{1}{R_A}\right)$$

The final angle $\theta_B$ is

$$\theta_B = \theta(s = L) = \frac{1}{2}\left(\frac{1}{R_B} + \frac{1}{R_A}\right) L + \theta_A$$

This corresponds to a curvature at the end equal to

$$\frac{1}{R_B} = 2\frac{\theta_B - \theta_A}{L} - \frac{1}{R_A}$$

while the length of the clothoid $L$ is

$$L = \frac{2(\theta_B - \theta_A)}{\frac{1}{R_A} + \frac{1}{R_B}}$$

The last three equations can be used to find any of $\theta_A$, $\theta_B$ or $L$, given the other two. Once the constants $k_1$ and $k_2$ are known, $\theta(s)$ is determined and the coordinates $x(s)$ and $y(s)$ can be found by integration:

$$x(s) = \int_0^s \cos\big(\theta(\zeta)\big)d\zeta + x_A$$

$$y(s) = \int_0^s \sin\big(\theta(\zeta)\big)\,d\zeta + y_A$$

The above integrals are in general to be determined numerically.

In the case analyzed here (see Fig. 2), $1/R_A = 0$, $\theta_A = 0$ and $\theta_B = 90°$, that implies

$$\theta(s) = \frac{1}{2}\frac{\pi}{L^2}s^2$$

$$x(s) = \int_0^s \cos\left(\frac{1}{2}\frac{\pi}{L^2}\zeta^2\right)d\zeta$$

$$y(s) = \int_0^s \sin\left(\frac{1}{2}\frac{\pi}{L^2}\zeta^2\right)d\zeta$$

The length $L$ can be found imposing $y(s = L) = 1$. The numerical solution is reported in Fig. 10 and is coincident with the one of [9].

In this case, there are no free parameters left to tune to minimize the energy, since they are all used to impose the boundary conditions. The horizontal span $h$ of the arc is larger of both the elliptic and the superelliptic cases, while the total strain energy is in between them (closer to the optimized superelliptic solution).

The curvature as a function of $s$ and $x$ is reported in Fig. 11. The function $k(s)$ is linear, since this is the very definition of the clothoid, while $k(x)$ is almost linear for a good three quarters of the arc. A smooth transition with the straight part is therefore in place. Moreover, this transition can be easily manipulated in the case of partial (less than 90°) arcs, by working on the parameters $k_1$ and $k_2$. Also, transitions other than the linear one can be straightforwardly imposed by changing the assumed $k(s)$ relation, obtain a sort of generalized clothoid. For this reason the derivation for the classical clothoid is reported in detail above.

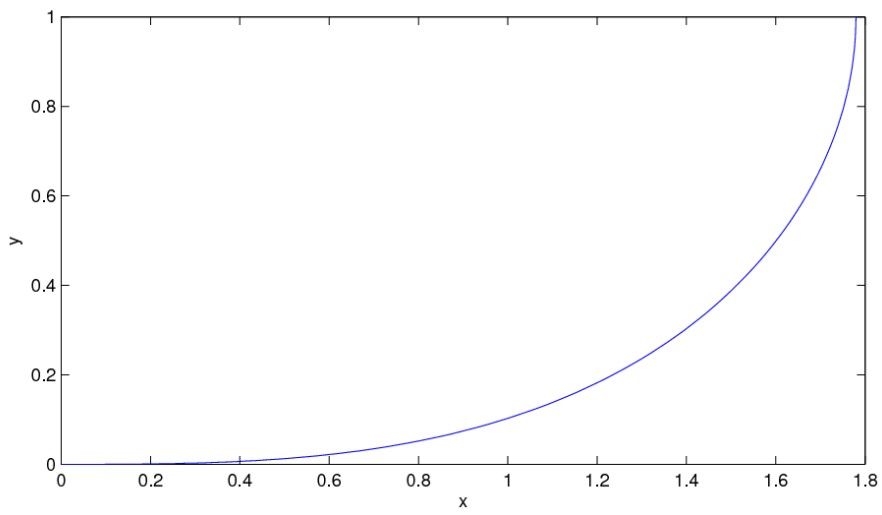


$$h = 1.7795$$

$$L = 1.4526 \cdot \frac{\pi}{2}$$

$$E = 0.9179 \cdot \frac{\pi}{2}$$

$$R_{min} = \frac{L}{\pi} = = 0.7263$$

$$R_{max} = \infty$$

Figure 10. Clothoid.

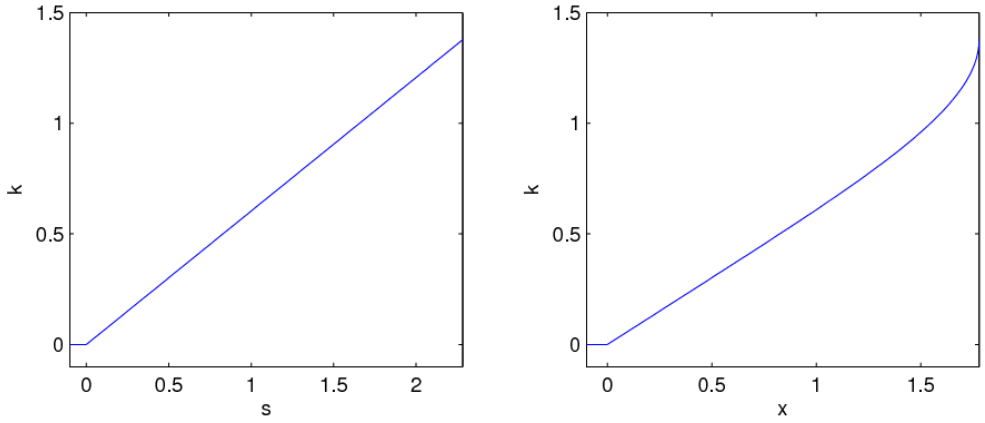


Figure 11. Curvature $k(s)$ and $k(x)$ for the clothoid.

## 6. Least energy convex curve

Is it possible to lower the total strain energy below that of the superelliptic case? The answer is yes, although not by much. The interesting part is not only to find the minimum energy curve, but also to analyze its minimum and maximum bending radii, as well as its general shape. The solution is known (see [8] and [9], for example), but a full derivation is reported next, as it will be used – with minor modifications – to handle the case of minimum energy "blocks". If in the previous cases (for example, the superelliptic arc) the optimization can be performed with respect to some real variables, since the shape of the curve is assumed, now the very curve is unknown: in a way, now it is like having infinite degrees of freedom to tune. In fact, the solution uses techniques of variational calculus.

The first assumption is to consider a convex curve, since this is the case of interest for winding coil ends. Therefore, the curvature has a fixed sign. So, the tangent angle $\theta$ along the arc is monotonic with the distance $s$ and it can serve as a parameter for the curve [10]. Since

$$ds = R(s)d\theta$$

the total energy is

$$E = \int_0^L [k(s)]^2 ds = \int_{\theta_A}^{\theta_B} \frac{1}{[R(\theta)]^2} R(\theta) d\theta = \int_{\theta_A}^{\theta_B} \frac{1}{R(\theta)} d\theta \quad \Rightarrow \quad E = \int_0^{\pi/2} \frac{1}{R} d\theta$$

which is a functional of *R*.

Since

$$dx = R(\theta)\cos\theta \, d\theta$$

$$dy = R(\theta)\sin\theta \, d\theta$$

then

$$\int_{\theta_A}^{\theta_B} R(\theta)\cos\theta \, d\theta = x_B - x_A \quad \Rightarrow \quad \int_0^{\pi/2} R\cos\theta \, d\theta = h$$

$$\int_{\theta_A}^{\theta_B} R(\theta)\sin\theta \, d\theta = y_B - y_A \quad \Rightarrow \quad \int_0^{\pi/2} R\sin\theta \, d\theta = 1$$

These two constraints can be incorporated to form a new functional *J* via two Lagrange multipliers, $\lambda_1$ and $\lambda_2$, as

$$J = \int_0^{\pi/2} \left[\frac{1}{R} + \lambda_1\left(R\cos\theta - \frac{2}{\pi}h\right) + \lambda_2\left(R\sin\theta - \frac{2}{\pi}\right)\right] d\theta$$

An extremal value of *J* can found applying the Euler-Lagrange equation, as

$$\frac{\partial}{\partial R}\left[\frac{1}{R} + \lambda_1 R\cos\theta + \lambda_2 R\sin\theta\right] = 0$$

that is,

$$-\frac{1}{R^2} + \lambda_1\cos\theta + \lambda_2\sin\theta = 0 \quad \Rightarrow \quad R = \frac{1}{\sqrt{\lambda_1\cos\theta + \lambda_2\sin\theta}}$$

having assumed positive radius of curvature. The multiplier $\lambda_1$ is easily found from the boundary conditions, as

$$\frac{1}{R(\theta = 0)} = 0 = \sqrt{\lambda_1 \cdot 1 + \lambda_2 \cdot 0} \quad \Rightarrow \quad \lambda_1 = 0$$

For $\lambda_2$, the following relation can be used

$$\int_0^{\pi/2} R\sin\theta\, d\theta = \int_0^{\pi/2} \frac{1}{\sqrt{\lambda_2 \sin\theta}} \sin\theta\, d\theta = \int_0^{\pi/2} \frac{\sqrt{\sin\theta}}{\sqrt{\lambda_2}}\, d\theta = \frac{1}{\sqrt{\lambda_2}} \Gamma^2(3/4) \sqrt{\frac{2}{\pi}} = 1$$

$$\int_0^{\pi/2} R\cos\theta\, d\theta = \int_0^{\pi/2} \frac{1}{\sqrt{\lambda_2 \sin\theta}} \cos\theta\, d\theta = \frac{1}{\sqrt{\lambda_2}} 2 = h$$

Hence,

$$\frac{1}{\sqrt{\lambda_2}} = \frac{h}{2}$$

and

$$h = \frac{\sqrt{2\pi}}{\Gamma^2(3/4)} \approx 1.6693$$

It can be shown that the length $L$ is

$$L = \frac{1}{2} \frac{\Gamma^4(1/4)}{(2\pi)^2} \approx 2.1884$$

and the corresponding integrated strain energy is

$$E = \frac{(2\pi)^3}{\Gamma^4(1/4)} \approx 1.4355$$

The maximum and minimum radii of curvature are in correspondence of the beginning and end of the curve, as

$$R_{min} = R_B = \frac{h}{2} \approx 0.8346, \qquad R_{max} = R_A = \infty$$

This stationary solution of the functional $J$ can be shown to be a minimum of $J$: therefore, the above equations correspond to the least energy (convex) curve. To find the coordinates $x$ and $y$ of the curve, it is enough to solve

$$\frac{d\theta}{ds} = \frac{2}{h} \sqrt{\sin\theta}$$

from $\theta = 0$ to $\theta = \pi/2$. The $x$ and $y$ coordinates of the curve are then obtained from

$$x(\theta) = \int_0^{\theta} \cos\big(\varphi(t)\big)\, dt$$

$$y(\theta) = \int_0^{\theta} \sin\big(\varphi(t)\big)\, dt$$

where $\varphi(t)$ is the angle along the curve.

The first ordinary differential equation above has a solution in terms of elliptic integrals, but can also be resolved numerically. Since $d\theta/ds(\theta = 0) = 0$, at least the first integration step needs to use an implicit scheme. The solution is shown in Fig. 12, where $\theta$ has been solved using the Euler implicit scheme for the first step, and the classical 4th order explicit Runge-Kutta for the others; $x$ and $y$ are obtained from trapezoidal integration.

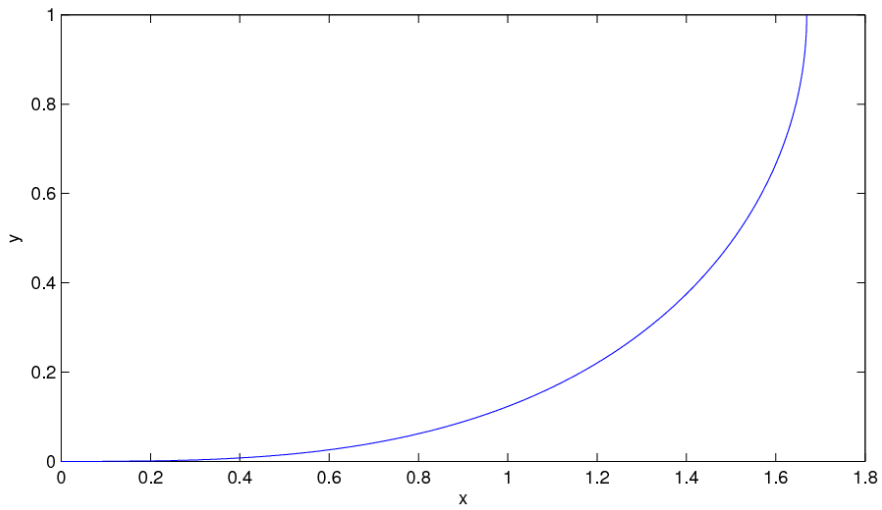


$$h = 1.6693$$

$$L = 1.3932 \cdot \frac{\pi}{2}$$

$$E = 0.9139 \cdot \frac{\pi}{2}$$

$$R_{min} = \frac{h}{2} = = 0.8346$$

$$R_{max} = \infty$$

Figure 12. Least energy convex curve.

This solution is coincident with the one reported in [9], although the actual solution scheme employed is different.

The curvature along the distance $s$ and horizontal coordinate $x$ is reported in Fig. 13.

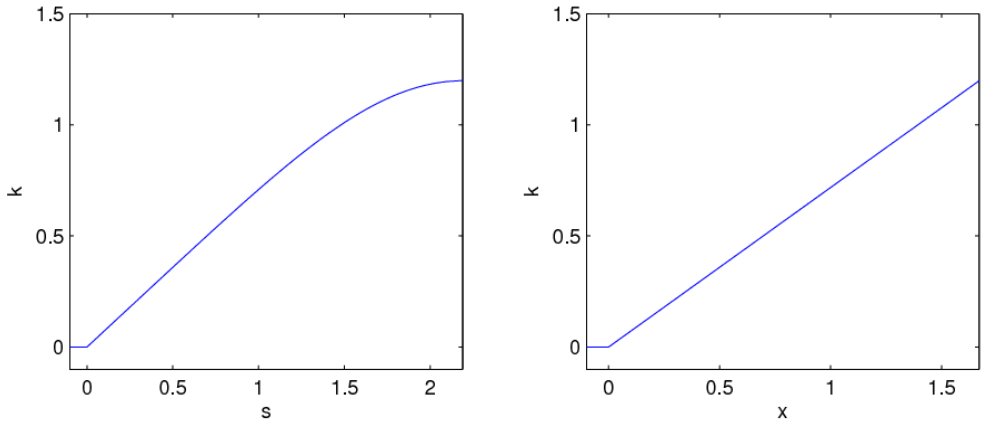


Figure 13. Curvature $k(s)$ and $k(x)$ for the least energy curve.

Clearly $k(x)$ is linear: this can be proven rigorously from the above equations. The superelliptic arc, with just three degrees of freedom, was able to approximate the least energy curve rather well, as can be seen from all the values ($L$, $h$, $E$, $R_{min}$ and $R_{max}$) and by the shape of the arc itself. Furthermore, its tendency of exhibiting an almost linear $k(x)$ is now explained.

## 7. Minimum energy curves of fixed length

A closely related problem is that of finding the minimum energy curve of fixed length. If the analysis is limited to convex curves, the solution can be found as in the previous section, with an additional constraint:

$$\int_{\theta_A}^{\theta_B} R(\theta)d\theta = L \qquad \Rightarrow \qquad \int_{0}^{\pi/2} Rd\theta = L$$

Therefore, a third Lagrange multiplier $\lambda_3$ appears in the functional $J$ to be minimized, as

$$J = \int_{0}^{\pi/2} \left[\frac{1}{R} + \lambda_1\left(R\cos\theta - \frac{2}{\pi}h\right) + \lambda_2\left(R\sin\theta - \frac{2}{\pi}\right) + \lambda_3\left(R - \frac{2}{\pi}L\right)\right] d\theta$$

and the differential equation for $d\theta/ds = 1/R$ can be derived from

$$\frac{\partial}{\partial R}\left[\frac{1}{R} + \lambda_1 R\cos\theta + \lambda_2 R\sin\theta + \lambda_3 R\right] = 0$$

Instead of using this approach, the minimum energy curve of a given length $L$ can be also found exploiting the physics of the problem. A simple finite element code is in fact capable of finding such curves. In fact, using a nonlinear beam element, capable of large displacements, and imposing the proper constraints, the least energy curve of given length is readily found. This has two advantages: also non-convex arcs can be found, and the special case of least energy convex curve can be checked.

A set of solutions is presented in Fig. 14, where the commercial finite element code ANSYS [12] is used. The code developed for this problem is included in the Appendix. The colours in Fig. 14 are values of (local) strain energy and they show areas of high / low bending radius. The various curves are found fixing several lengths, as follows:

- $L$ = 1.5708 → $E$ = 1.5708 (circular arc)
- $L$ = 0.85×2.1884 → $E$ = 1.4463
- $L$ = 2.1884 → $E$ = 1.4355 (least energy convex curve)
- $L$ = 1.3×2.1884 → $E$ = 1.4152
- $L$ = 1.7×2.1884 → $E$ = 1.3254
- $L$ = 2.0×2.1884 → $E$ = 1.2424
- $L$ = 2.5×2.1884 → $E$ = 1.1084

The results for the circular arc and the least energy convex curve are consistent with the analytical ones of the previous sections. If non-convex curves are considered, the total strain energy $E$ can be further lowered; it can be shown that $E$ can be lower than any given fixed value, if the length $L$ is properly increased and non-convexity is allowed. These non-convex long curves are of course not interesting for winding purposes.

Furthermore, the least energy convex curve ($L$ = 2.1884, $h$ = 1.6693) is also the only one that starts off with zero curvature. If shorter curves are sought ($L$ < 2.1884, $h$ < 1.6693), then these will involve a discontinuity on the second derivative in point A. If longer curves ($L$ > 2.1884, $h$ > 1.6693) are considered, the radius of curvature will undergo a sign change.

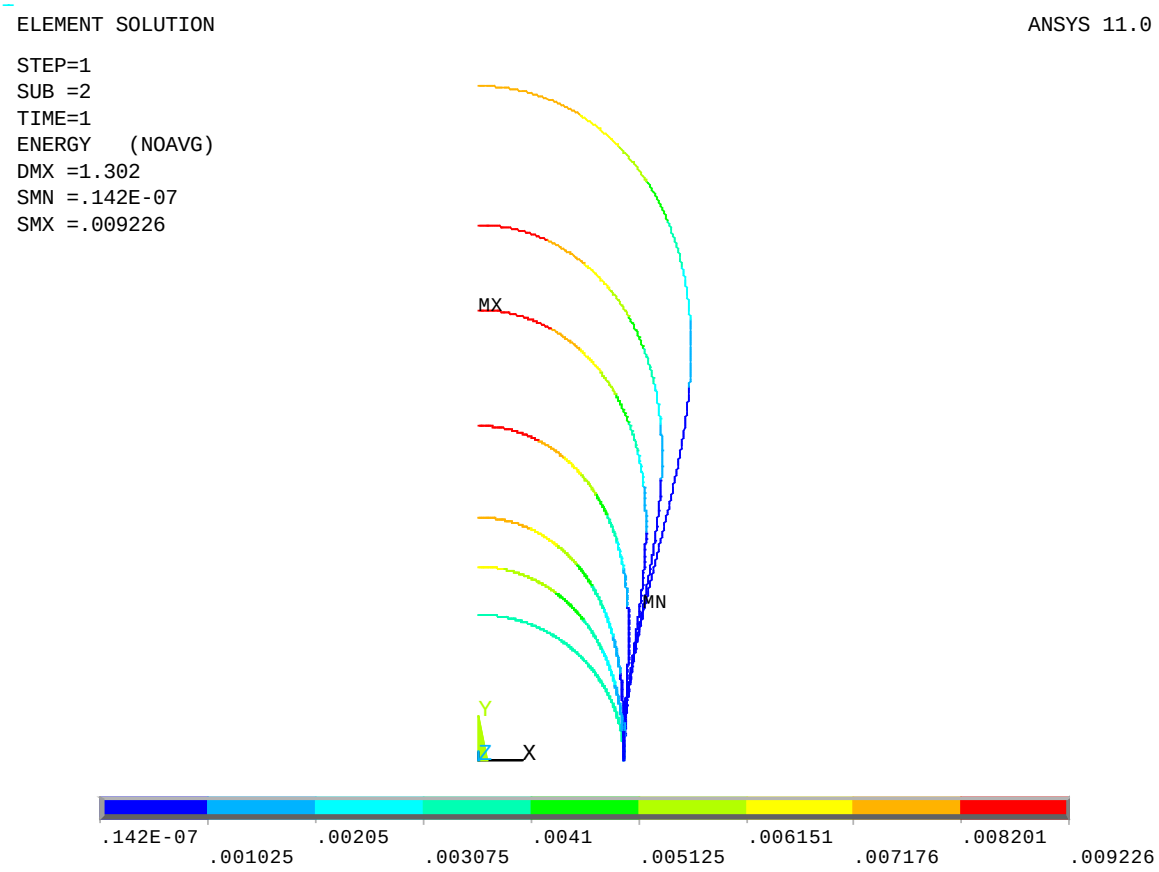


Figure 14. Minimum energy curves of fixed lengths.

## 8. Baseline for minimum energy blocks

All the results presented in the previous sections concentrate on a single curve and, in particular, on the elastic strain energy / radius of curvature along it. What happens when instead of a single turn a block of $N$ turns, with equal spacing $d$, is considered?

This problem can be tackled analytically in the same way as the single least energy curve. No straightforward approach to cast it in a form solvable with a finite element code seems apparent.

Consider – as shown in Fig. 15 – two infinitesimal pieces of cable with an offset equal to $d$. This dimension is in practice the thickness of the insulated cable. The inner one has length $ds$ and radius of curvature $R$, so that its infinitesimal strain energy is

$$dE_{inner} = \frac{1}{R^2} ds = \frac{1}{R} d\theta$$

For the outer, of length $ds'$ and radius of curvature $R+d$, the local energy is written as

$$dE_{outer} = \frac{1}{(R+d)^2} ds' = \frac{1}{R+d} d\theta$$

Now, $d$ is a constant, hence integration returns

$$E_{inner} = \int_{\theta_A}^{\theta_B} \frac{1}{R} d\theta$$

$$E_{outer} = \int_{\theta_A}^{\theta_B} \frac{1}{R+d} d\theta$$

and so

$$E_{inner} + E_{outer} = \int_{\theta_A}^{\theta_B} \left[\frac{1}{R} + \frac{1}{R+d}\right] d\theta$$

Hence, the total strain energy of the block of two cables can be expressed as a functional involving only $R(\theta)$. In general, if a total of $N$ turns is present, each spaced by $d$, the energy is

$$E_{total} = \int_{\theta_A}^{\theta_B} \left[\frac{1}{R} + \frac{1}{R+d} + \frac{1}{R+2d} + \cdots\right] d\theta = \int_{\theta_A}^{\theta_B} \sum_{i=0}^{N-1} \frac{1}{R+id} d\theta$$

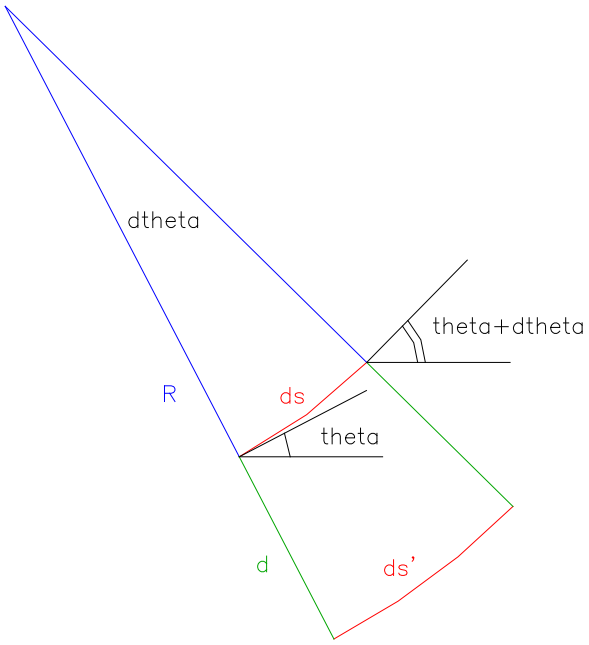


Figure 15. Two infinitesimal lengths of cable with an offset equal to $d$.

The constraints on the $x$ and $y$ coordinates are applied using Lagrange multipliers as before. If a 90° arc is considered, the functional to be minimized is

$$J = \int_0^{\pi/2} \left[ \sum_{i=0}^{N-1} \frac{1}{R + id} + \lambda_1 \left( R\cos\theta - \frac{2}{\pi} h \right) + \lambda_2 \left( R\sin\theta - \frac{2}{\pi} \right) \right] d\theta$$

Applying the Euler-Lagrange equation, the function $R(\theta)$ needs to satisfy

$$\lambda_1 \cos\theta + \lambda_2 \sin\theta = \sum_{i=0}^{N-1} \frac{1}{(R + id)^2}$$

that is

$$\lambda_1 \cos\theta + \lambda_2 \sin\theta = \sum_{i=0}^{N-1} \frac{1}{\left( \frac{ds}{d\theta} + id \right)^2}$$

The above is a differential equation where the term $d\theta/ds$ is not explicitly given. However, it can still be solved numerically, for example using an Euler implicit scheme of integration. That is, if the length $s$ along the curve is discretized as

$$s_j = j\Delta s, \qquad j = 0,1,\dots, L/\Delta s$$

then the corresponding tangent angles $\theta_j$ can be found as

$$\lambda_1 \cos\theta_j + \lambda_2 \sin\theta_j = \sum_{i=0}^{N-1} \frac{1}{\left( \frac{\Delta s}{\theta_j - \theta_{j-1}} + id \right)^2}, \qquad j = 1,\dots, L/\Delta s$$

with $\theta_0 = 0$ since the baseline has to start with horizontal tangent. The above nonlinear equation in $\theta_j$ can be solved at each step in a few iterations. The distance step $\Delta s$ should be chosen small enough, since errors in $\theta$ can easily add up, due to the accuracy of the solution scheme.

The boundary conditions impose

$$\frac{1}{R(\theta = 0)} = 0 \quad \Rightarrow \quad \lambda_1 = 0$$

$$\frac{1}{R(\theta = \pi/2)} = R_B \quad \Rightarrow \quad \lambda_2 = \sum_{i=0}^{N-1} \frac{1}{(R_B + id)^2}$$

With these conditions, the use of an implicit scheme for at least the first step is essential (as before), otherwise the trivial solution $\theta_j = 0$ would be found. Since $R_B$ is not known, the length of the curve $L$ and the parameter $\lambda_2$ need to be tuned (iteratively) as to reach the final point at a vertical distance equal to 1 and with vertical tangent.

A solution obtained fixing $d = 0.05$ and $N = 10$ is shown in Fig. 16, together with the reference circular arc and the (single) minimum energy curve. For this case, $\lambda_2 = 9.9923$ and

$L$ = 2.3025. It can be concluded that when blocks of different number of turns $N$ are considered, the least energy baseline will change, as shown in the figure. It is also clear that if a large block is split in two, allowing the separate design of two different baselines (this is the case when end spacer are added, for example) then the total strain energy can be lowered. The extreme case – rather unpractical – would be to add a spacer in between every single turn, so that each cable could lay on the most suitable geometry.

The above considerations can be straightforwardly extended when an elliptic or superelliptic baseline is considered. In that case, the procedure is much more direct, as no solution of differential equations is required. In fact, a unidimensional minimization (with respect to the variable $h$) is enough for the ellipse, while for the superellipse a tuning of three parameters ($h$, $n$ and $m$) is needed.

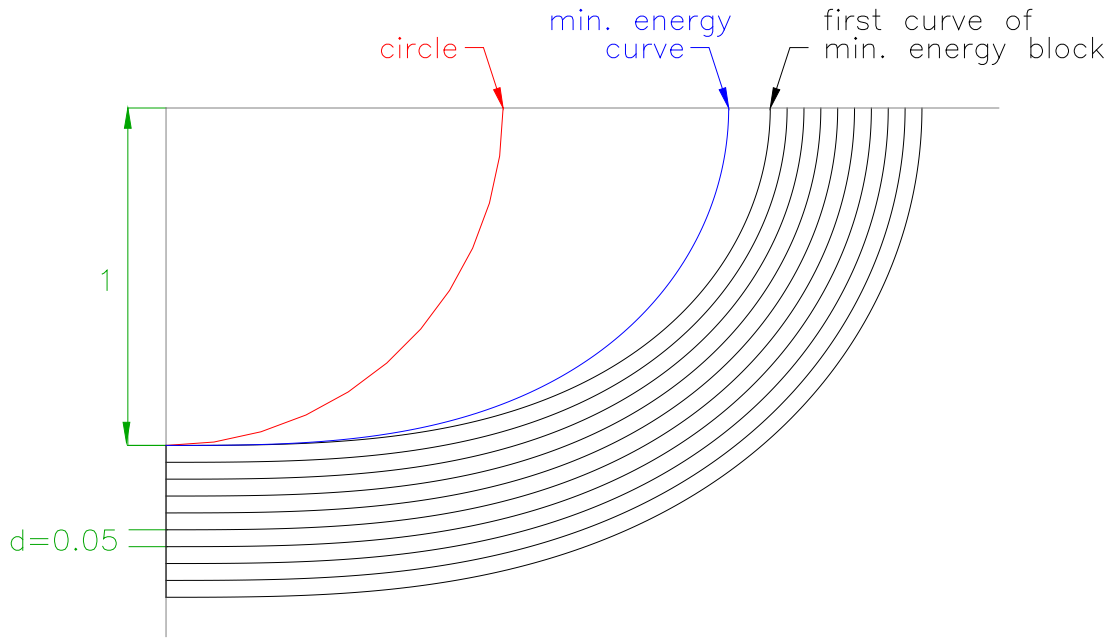


Figure 16. Baseline minimizing the total energy for $d$ = 0.05, $N$ = 10.

## 9. Conclusions

A comparison between several curves is reported next. In Fig. 17, the shapes of the curves are plotted side by side and in Table 1 a summary of their properties is gathered. From a purely geometric perspective, several points can be inferred:

- the circular arc is the simplest solution, though it involves the higher total strain energy *E*, as well as the largest discontinuity on curvature where the arc meets the straight section

- choosing the proper ellipse, it is possible to lower *E* as well as the curvature jump; however, the minimum radius of curvature, at the end of the curve, is decreased and the total horizontal length of the arc is increased

- the properly tuned superellipse provides a solution that connects smoothly to the straight part, eliminating discontinuities in curvature that may be hard to impose to a real cable. Furthermore, the energy *E* is almost minimized, while the minimum radius of curvature is kept relatively high

- the clothoid is relatively easy to draw to obtain smooth transitions, but its performance in terms of integrated energy, minimum radius of curvature and length are less satisfactory than the other options. However, this solution remains attractive when partial arcs need to be designed and the curvature change is to be controlled

- the minimum energy curve has an *E* that is only slightly lower than, for example, the superelliptic arc. This small gain is paid by an increased length. This curve is more cumbersome to obtain analytically, though it can be derived from an elementary finite element simulation.

Since a mathematical description of the various options is detailed here, it is now possible to further analyze actual windings exploiting these transition curves (such an activity is planned together with CEA Saclay, see [13]).

Furthermore, these geometries can also be used for other simulations. In particular, the code ROXIE [14] could be modified to perform magnetic analyses using these baselines.

Although the analysis presented here is planar, an extension to the three dimensional case is possible. For example, Fig. 18 shows how a flared end of a block dipole could look like, using the concepts detailed in the previous sections. The half cylinder is simply drawn as a reference. The blocks (two layers) first experience a hard way bend, following a double clothoid, so that the curvature is varied from 0 to a given value to 0 again. In the meanwhile, while the second clothoid is about to end, the easy way bend starts, following a clothoid again. Most of the easy way bend takes place on a plane inclined with respect to the midplane of the dipole. A clothoid is used since tuning the change in curvature is immediate; however, other baselines (e.g., superelliptic) could be implemented.

Table 1. Summary of curves and their properties.

| curve | $h$ | $L$ | $E$ | $R_{min}$ | $R_{max}$ | smooth transition |
|---|---|---|---|---|---|---|
| circle | 1 | 1.5708 | 1.5708 | 1 | 1 | no |
| ellipse | 1.3204 | 1.8311 | 1.4674 | 0.7573 | 1.7435 | no |
| superellipse | 1.6189 | 2.0857 | 1.4357 | 0.844 | ∞ | yes |
| clothoid | 1.7795 | 2.2818 | 1.4418 | 0.7263 | ∞ | yes |
| min. energy curve | 1.6693 | 2.1884 | 1.4355 | 0.8346 | ∞ | yes |

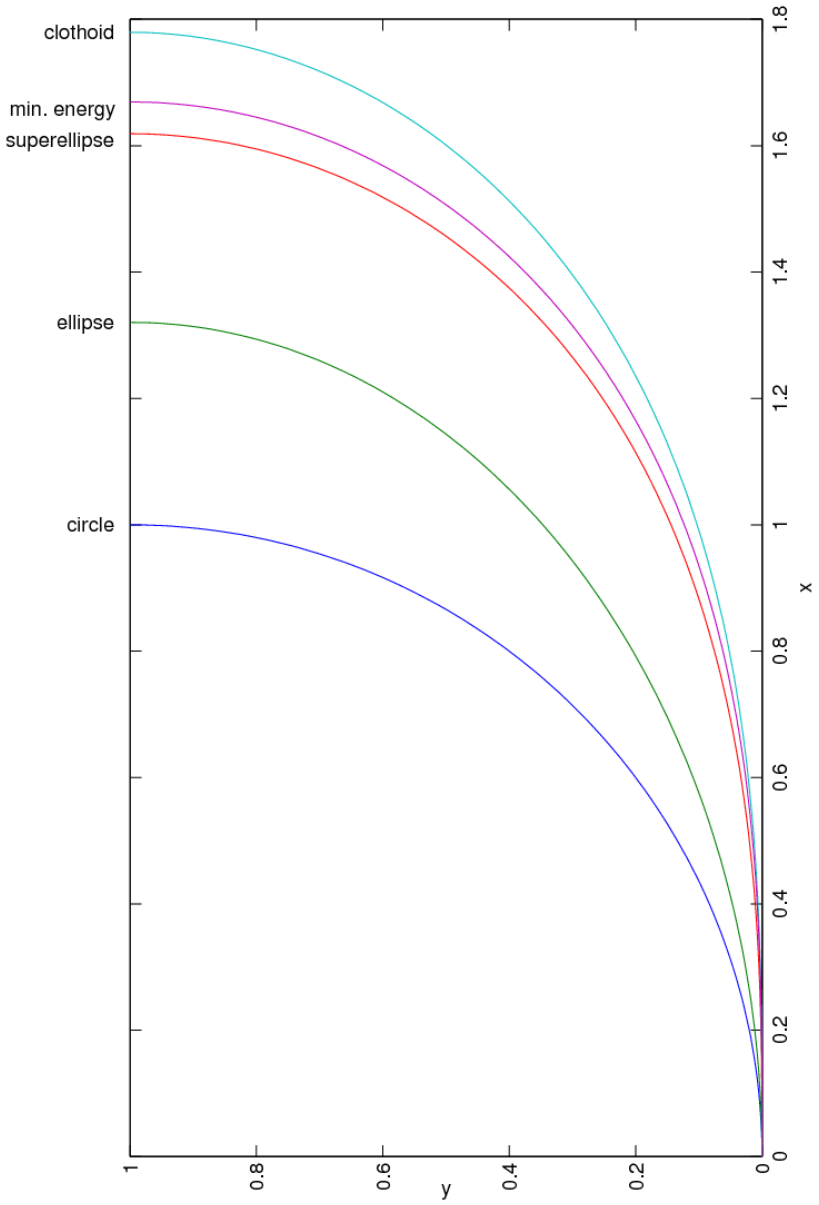


Figure 17. Shapes of various curves herein proposed.

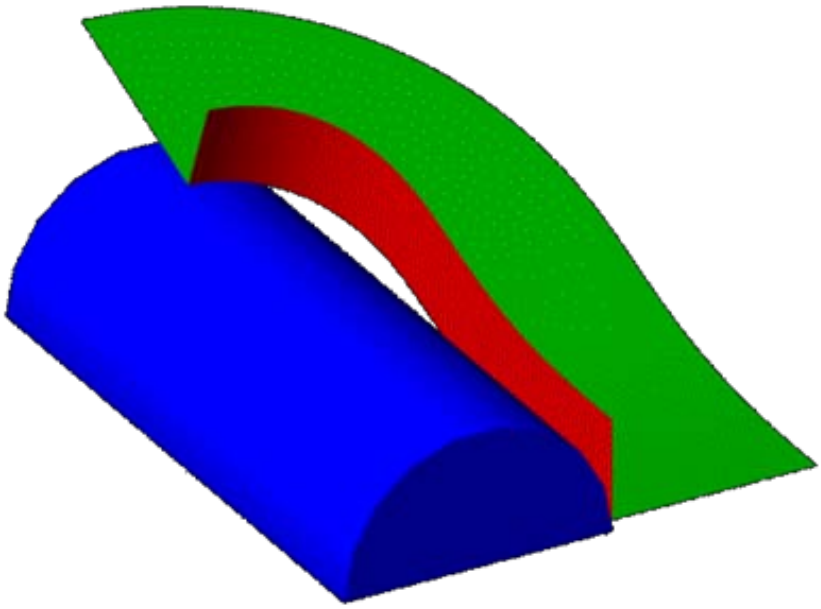

Figure 18. Flared end possibility for a block dipole.

## References


[1] K. Chow *et al*., "Fabrication and test results of a $Nb_3Sn$ superconducting racetrack dipole magnet," in *PAC-1999*.

[2] V. S. Kashikhin *et al*., "Development and test of single-layer common coil dipole wound with reacted $Nb_3Sn$ cable," *IEEE Trans. Appl. Supercond.*, vol. 14, p. 353, Jun. 2004.

[3] L. Chiesa *et al*., "Magnetic field measurements of the Nb3Sn common coil dipole RD3c," in *PAC-2003*.

[4] P. Ferracin *et al*., "Mechanical analysis of the Nb3Sn dipole magnet HD1," *IEEE Trans. Appl. Supercond.*, vol. 15, p. 1119, Jun. 2005.

[5] F. Regis *et al.*, "Mechanical design of the Short Model Coil Dipole magnet," in *MT-21*, Oct. 2009.

[6] P. Ferracin *et al*., "Recent test results of the high field $Nb_3Sn$ dipole magnet HD2," in *MT-21*, Oct. 2009.

[7] P. Ferracin, private communication.

[8] L. Euler, "De curvis elasticis," appendix of *Methodus inveniendi lineas curvas maximi minimive proprietate gaudentes, sive solutio problematis isoperimetrici lattissimo sensu accepti*, 1744.

[9] B. K. P. Horn, "The curve of least energy," *ACM Trans. Math. Software*, vol. 9, p. 441, Dec. 1983.

[10] M. Kallay, "Plane curves of minimal energy," *ACM Trans. Math. Software*, vol. 12, p. 219, Sept. 1986.

[11] MATLAB User's Guide, 2006, The MathWorks Inc.

[12] ANSYS 11.0 Documentation, ANSYS, Inc.

[13] Minutes of the Magnet Pre-design Working Group meeting (within task 3 of EuCARD WP7-HFM) held at CERN Dec. 8, 2009.

[14] S. Russenschuck, *Electromagnetic design and mathematical optimization methods in magnet technology*. [Online] Available: http://cern.ch/russ, 3rd ed. Feb. 2006

## Appendix

The code to obtain the least energy curve of given length is given below; ANSYS v. 11.0 is used.

```
/prep7

L = 2.18843961   ! length

! keypoints
k,1,1,0
k,2,1,L

! line
l,1,2

! divide the line in 400 parts
esize,,400

mp,ex,1,2.      ! elastic modulus equal to 2
mp,prxy,1,0.3   ! Poisson ratio (not essential)

et,1,beam3      ! Euler-Bernoulli beam element
r,1,1e5,1.,1.    ! much stiffer axially then in bending, so length is
const.

lmesh,all

! impose displacements on point A
dk,1,ux,0
dk,1,uy,0
dk,1,rotz,0

! impose displacements on point B
dk,2,ux,-1
dk,2,rotz,acos(-1)/2



/solu

nlgeom,1                ! activate geometric nonlinearities (important)
cnvtol,u,,0.000001,2,,  ! put a tighter convergence criterion

solve



/post1

pldisp,2

etable,energy,sene,elastic
pletab,energy,noav     ! plot the elastic strain energy
ssum
```